ACS OMEGA

Open Access

http://pubs.acs.org/journal/acsodf

Article

Analysis of the Formation Mechanism of Hydrogen Sulfide in the 13# Coal Seam of Shaping Coal Mine

Chunming Ai, Siqi Wang,* Pingping Sun, Shuyu Zhao, and Xiaozhi Mu

Cite This: *ACS Omega* 2024, 9, 2980−2987

Read Online

ACCESS | Metrics & More | Article Recommendations

ABSTRACT: In order to accurately predict the law of occurrence and migration of hydrogen sulfide (H_2S) in the underground and effectively solve the problem of excessive concentration of H_2S gas, laboratory experiments on the content of various forms of sulfur in coal, sulfur isotopes, thermal evolution history, and coal seam water samples were carried out by applying the theories of coal mine geology, microbiology, and analytical chemistry, and based on the experimental results, the cause of H_2S gas was explored. Through the analysis of the geological conditions of the coal seam mined, it can be seen that the coal mine experienced the alternation of marine and continental phases in the process of coal formation and that there was no magma intrusion. The experimental results showed that iron sulfide in coal accounts for 73.25% of the total sulfur, indicating that the coal seam was rich in pyrite. The results of the isotope test showed that the sulfur isotopes in coal samples were all negative, indicating that the sulfur isotope fractionation in coal was large, the loss was serious, and the coal seam was greatly affected by seawater. According to the experimental results of vitrinite reflectance, it can be concluded that the highest temperature during the thermal evolution of the coal seam is 108.12 °C, which has not reached the temperature condition of sulfate thermochemical reduction. Comparing the concentration of acid ions in coal seam water and tap water, it was found that the concentration of SO_4^{2-} in coal seam water is low, while the concentration of HCO_3^- is high. According to the experimental results and theoretical analysis, the H_2S gas in the high-sulfur coal mine was caused by microbial sulfate reduction. Finally, the transformation path of sulfur in the coal seam was deduced and analyzed. The results showed that sulfur in coal is positively correlated with H_2S gas concentration.

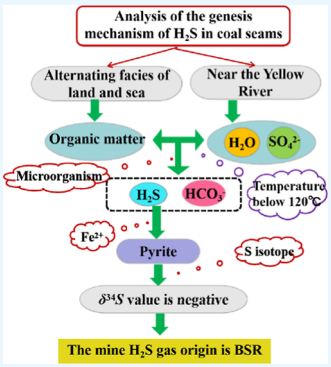

1. INTRODUCTION

Hydrogen sulfide gas (H_2S) is a common toxic and harmful gas in coal mines. It is heavier than air and often accumulates in low depressions.[1−3] H_2S is extremely soluble in water, and its aqueous solution is acidic and highly corrosive to metal equipment in the mine. H_2S concentration of 100 ppm, 15 min will cause human olfactory paralysis; at a concentration of 1500 ppm, the human body immediately smells like a dead body. In coal mining, abnormal emissions and disaster accidents caused by H_2S enrichment in coal seams occur constantly at home and abroad, posing a major threat to the occupational health and life safety of coal mine workers.[4−6]

A relatively obvious smell of H_2S appeared during mining in the Shaping coal mine of Shanxi. After testing, it was found that the content of H_2S in the 13# coal seam seriously exceeded the standard. The content of H_2S in coal seam water was as high as 2000 ppm, and the content in roadway air was 30 ppm. Article 135 of the "Coal Mine Safety Regulations" (2022) stipulates that the H_2S volume fraction shall not exceed 6.6 ppm.[7] In order to ensure the lives and health of underground workers, corresponding measures must be taken to control excess H_2S. At present, the methods commonly used in mines at home and abroad include alkali injection by drilling holes, strengthening ventilation, changing ventilation mode, enhancing personal protection, etc.[8−10] Research on the formation mechanism of H_2S in coal seams can help to understand its physical and chemical generation process, master and predict the distribution law of H_2S in underground mines, and provide a basis for effectively preventing and controlling H_2S disasters in coal mines.

The origin of H_2S can be roughly divided into five types:[1] biodegradation, bacterial sulfate reduction (BSR), thermochemical decomposition, thermochemical sulfate reduction (TSR), and magmatic activity. The cause of biodegradation is the process of forming H_2S under the dominance of corruption. The scale of the H_2S generated is generally small, and the storage conditions are relatively harsh. BSR occurs in an anaerobic environment created by underground coal seams and the surrounding rocks. The reducing bacteria absorb sulfate in coal, oxidize organic matter and compounds in the coal, and obtain

Received: November 14, 2023
Revised: December 5, 2023
Accepted: December 21, 2023
Published: January 3, 2024

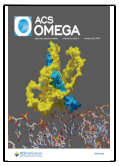

the energy needed for survival. The cause of thermochemical decomposition is that the sulfur-containing heterocyclic ring of sulfur-containing organic matter breaks under high temperature and high pressure to produce H_2S, which is generally found in oil and natural gas but hardly occurs in coal mines. TSR occurs in a high-temperature environment where sulfates, sulfur-containing compounds, and other organic compounds are reduced to H_2S gas. The released H_2S accumulated in the coal seam. Magmatic activity refers to the process by which H_2S and other volatile products in underground magma enter the coal seam through cracks or pores in the formation. The most common origins are BSR, TSR, and magmatic activity.

At present, the genesis of H_2S in coal seams is mainly explored from the aspects of the geological environment, sulfur isotopes, and geothermal history at home and abroad. Hosseiny et al.[11] discussed thermal cracking, BSR, and deep migration and concluded that BSR was the main mechanism of H_2S generation in oilfield reservoirs. Yongjie et al.[12] introduced polyethylenimine into MOFs and found that it improved the adsorption performance of H_2S and achieved clean and efficient utilization of coal. de Oliveira Carneiro et al.[13] established a coke oven gas purification process model and evaluated solutions that can remove H_2S to a greater extent. Li et al.[14] studied the distribution of TSR and H_2S in the Sichuan Basin based on carbon isotope data and sulfur isotope data of solid bitumen, sulfide gas, and anhydrite. Xie et al.[15] analyzed the factors affecting the formation and enrichment of H_2S by considering geological factors such as the characteristics of combustion, gas composition, and groundwater geochemistry in the study area. The results showed that H_2S in the TSR was mainly formed in the coal fire area and its vicinity. Deng et al.[16] took coal samples from Shengli coal mine as the research object, isolated and purified sulfate-reducing bacteria (SRB) from mine water by the dilution plate anaerobic culture method, and found that temperature, environmental pH, and COD/SO_4^{2-} had significant effects on the production of H_2S. Gao et al.[17] discussed the adsorption mechanism of H_2S in coal and studied the occurrence state of H_2S in low-sulfur coal. Dao et al.[18] showed that the sulfur formed by BSR was mainly involved in early mineralization, and the addition of a large number of hydrothermal fluids in the later stage induced a TSR reaction. Yufen[19] speculated that H_2S in the Tiexin mine field in the Shanxi Province was caused by BSR and TSR based on the geological characteristics and stratigraphic deposition laws of the mine. Asaoka et al.[20] revealed the temporal and spatial distribution of sulfur forms in marine sediments in Osaka Bay, Japan, through the combined method of lead sulfide ribbon detection tube and X-ray absorption fine structure spectroscopy. Cheng et al.[21] showed that TSR was the main reason for the high H_2S content in carbonate reservoirs through the analysis of the physical properties and thermodynamic conditions of carbonate reservoirs. In order to determine the geothermal history of the coal seams, Dongna and Meiling[22] calculated the thermal evolution temperature per capita using vitrinite reflectance, providing strong evidence for the genetic analysis of H_2S gas in coal seams.

In recent years, the problem of H_2S overruns in coal mines has occurred from time to time, which has seriously affected the mining of coal resources. However, analysis of the causes of H_2S has not yet formed a system, and the depth and breadth of research are not sufficient. In this paper, the genetic analysis of the H_2S gas anomaly in the 13# coal seam of Shaping mine is taken as an example. The genetic mechanism of H_2S is explored from the aspects of pyrite content, thermal evolution history, and sulfur isotope content in coal by combining theory with experiment, which lays a foundation for effective control of H_2S disasters and safe and efficient mining of coal.

2. EXPERIMENTAL METHODS

2.1. Coal Quality Analysis. Coal was taken as samples at 6 positions, such as 500 and 800 m, in the glue transport passage of the 103 working faces of the 13# coal seam. This position was the fold (syncline or anticline) area of the coal seam, and the concentration of H_2S in the air of the roadway was relatively high, which was representative. A series of coal quality determination experiments were carried out by repeated testing of each sample three times and taking its average value. The sampling depth was 12−15 m. The specific locations are shown in Table 1 and Figure 1. The results of industrial and porosity analyses of coal samples are shown in Table 2.

Table 1. Sampling Locations of the Coal Samples

coal sample number	sampling point	sampling depth/m	sampling method	sampling quality/g
1	13103 glue transport through 500 m	12	drilling cuttings	100
2	13103 glue transport through 800 m	12	drilling cuttings	100
3	13103 glue transport through 900 m	15	drilling cuttings	100
4	13103 glue transport through 1300 m	15	drilling cuttings	100
5	13103 glue transport through 1500 m	15	drilling cuttings	100
6	13103 glue transport through 1800 m	12	drilling cuttings	100

2.2. Coal Vitrinite Reflectance Test. The vitrinite of coal is a maceral group formed by the humification and gelation of the lignocellulose tissue of coal-forming plants, which can directly reflect the metamorphic degree of coal. According to the method described in the "Sample preparation method for coal and rock analysis" (GB/T 16773-2008), the coal sample was broken to a particle size of less than 100 mm, mixed with the binder, heated, and pressed into a "coal brick", and the end face of the coal brick was ground and polished into a light sheet with a diameter of 3 cm and a thickness of 2 cm. The reflectivity was measured after 4 h in an oven at 35 °C.

According to the unit of the 0.05% reflectivity interval (half-order), the number of measurement points of half-order and their percentage of the total number are counted, as shown in Table 3. The average value (R_{max}) and standard deviation (S) of reflectivity are calculated, as shown in eqs 1 and 2.

$$R_{max} = \frac{\sum_{j=1}^{n} R_j X_j}{n} \quad (1)$$

$$S = \sqrt{\frac{\sum_{j=1}^{n} (R_j^2 X_j) - n\overline{R}^2}{n-1}} \quad (2)$$

where R_j—the middle value of the j order (or half-order) and X_j—the number of measuring points of order j (or half-order).

3. RESULTS AND DISCUSSION

3.1. Genesis and Occurrence Conditions of Hydrogen Sulfide in Coal Seam. According to the existing cases and

https://doi.org/10.1021/acsomega.3c09057
ACS Omega 2024, 9, 2980−2987

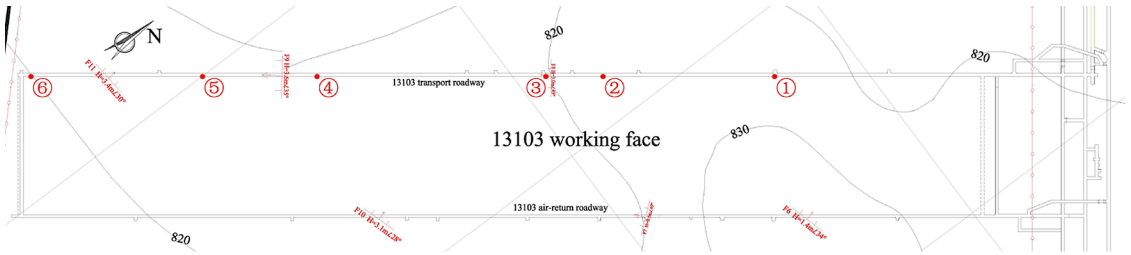

Figure 1. Location map of the coal sample (1:5000).

Table 2. Results of Industrial Analysis and Porosity Analysis of Coal Samples[a]

coal sample number	porosity/%	apparent relative density	A_{ad}/%	V_{ad}/%	M_{ad}/%	FC_{ad}/%	V_{daf}/%
1	2.18	2.24	50.76	22.06	1.08	26.10	45.81
2	0.52	1.93	69.33	16.12	0.92	13.63	54.18
3	3.95	1.70	42.42	26.71	1.28	29.59	47.44
4	0.82	2.42	70.08	14.66	1.00	6.26	70.08
5	1.77	2.22	69.32	15.00	1.08	14.60	50.68
6	2.44	1.60	26.98	25.38	1.90	45.74	35.69

[a]A_{ad}: mass fraction of the ash of the air-dry base, %; V_{ad}: mass fraction of the volatile fraction of the air-dry base, %; M_{ad}: mass fraction of the moisture of the air-dry base, %; FC_{ad}: mass fraction of the fixed carbon of the air-dry base, %; and V_{daf}: mass fraction of the volatile fraction of the dry ash-free base, %.

Table 3. Reflectivity of Each Coal Sample[a]

reflectivity/%	points number/n	frequency/%
[0.45, 0.50)	1	2
[0.50, 0.55)	13	26
[0.55, 0.60)	23	46
[0.60, 0.65)	11	22
[0.65, 0.70)	2	4
[0.70, 0.75)	0	0

[a]The macerals of the coal seam are organic components, mainly vitrinite and inertinite, and a small amount of exinite. Combined with the experimental data, the average value of the reflectivity R_{max} = 0.57%, and the standard deviation S = 0.036%.

distribution characteristics and theoretical analysis of coal seams in China,[23,24] it is known that BSR, TSR, and magmatic activity are the main causes of H_2S in coal seams.

The occurrence condition of BSR is that coal contains sulfate compounds, organic matter, and SRB at the same time. The organic matter in the coal generally exists in the sedimentary environment of marine facies and alternating marine and continental facies. Therefore, the marine-continental alternation in the process of coal formation is one of the prerequisites for the formation of BSR. The high content of pyrite in the coal seam is direct evidence of the formation of H_2S by BSR because H_2S produced by BSR is fixed by Fe^{2+} in the coal seam to form pyrite. Under the action of BSR, sulfate in the coal seam is reduced by bacteria to form sulfur, and the effect of sulfur isotope fractionation caused by bacterial dissimilation is more obvious. The average $\delta^{34}S$ value of pyrite in the coal seam is negative.

The necessary conditions for the occurrence of TSR are higher temperatures, sufficient hydrocarbon organic matter, and sulfate. The lower limit of temperature at which TSR occurs is 120 °C, which is a significant feature different from BSR. The S isotope fractionation value of H_2S formed by TSR is the smallest, and the $\delta^{34}S$ of sulfate and pyrite is generally positive, mostly above +10.0‰.[25]

The magma mainly contains sulfate minerals, such as pyrite and gypsum. There are two main reasons for judging whether H_2S in coal seams is derived from magmatic activity. One is to analyze whether the geological activity and volcanic activity are active after the coal-forming process in the mining area. The second is whether the sulfur isotope value of coal ranges from −5 to +5‰.[26] According to the geological background of the coal mine, it can be ruled out that the origin of H_2S in this mine is magmatic activity.

3.2. Analysis of Thermal Evolution History. The burial depth of the Shaping mine is below 1500 m. In the range of 20−30 m below the surface of the coal mine, the ground temperature is between 12.6 and 15.9 °C, which belongs to the constant temperature zone of ground temperature. Below 30 m from the surface, it belongs to the ground temperature warming zone, and the ground temperature gradient is 0.4−1.6 °C/100 m, with an average of 1.1 °C/100 m. The annual temperature range is 18.6−39.9 °C, which provides a suitable environment for the growth of reducing bacteria.

BSR occurs when the thermal evolution temperature is lower than 120 °C, and the lower limit of the thermal evolution temperature of TSR is 120 °C and generally occurs above 150 °C. Therefore, it is very important to determine the thermal evolution temperature of the coal seams for determining the genesis of H_2S. According to the relationship between the vitrinite reflectance and temperature, the thermal evolution temperature of the coal seam can be determined. The temperature relationship between the maximum paleo-geothermal temperature of the coal seam and the reflectance of the coal sample is as follows[27]

$$\ln R_0 = 0.0078T_{max} - 1.2 \quad (3)$$

where R_0 is the vitrinite reflectance of coal and T_{max} is the highest paleo-geothermal temperature.

Substituting the reflectivity of each stage in Table 3 into Formula 3, it can be calculated that the temperature evolution range of the coal seam in the coal-forming stage is between 51.47 and 108.12 °C. The middle value of the ancient ground temperature of the coal seam corresponding to the no. 1 to no. 6 coal samples is taken to make the ancient ground temperature and reflectivity change diagram of the coal seam; as shown in

https://doi.org/10.1021/acsomega.3c09057
ACS Omega 2024, 9, 2980−2987

Figure 2, it can be seen that the maximum temperature of the coal seam does not exceed 120 °C.

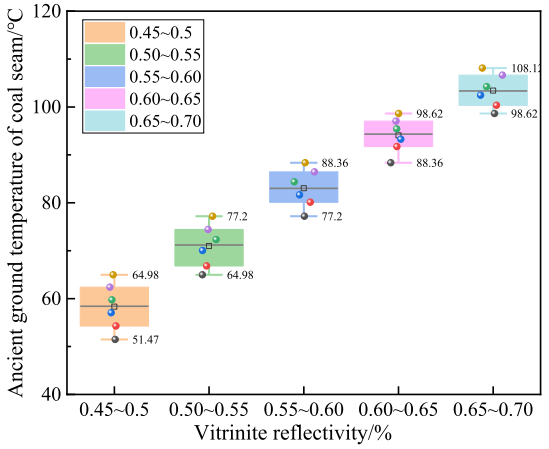

Figure 2. Plot of coal geotemperature with the reflectance of the mirror.

In summary, the temperature of the coal seam in the thermal evolution process of the 13# coal seam is lower than 120 °C, which does not reach the temperature condition of TSR. Therefore, the cause of TSR can be excluded.

3.3. Analysis of Pyrite in Coal. The coal seam 13# of the Shaping coal mine is located in the Taiyuan Formation of the Upper Carboniferous System. During the Late Carboniferous-Early Permian, seawater invaded from the western margin of Ordos, Benxi, and Huainan in three directions: north, northwest, and west, which caused two transgressions from north to south and then from south to north in the east of Lvliang Mountain in Shanxi block. The west side of Lvliang Mountain experienced at least one seawater intrusion. The 13# coal seam belonging to the Taiyuan formation is dominated by marine-continental transitional facies. In the sea-land alternation, large amounts of coal- and sulfur-forming organic matter are deposited in the coal seam. In the coal-forming stage, the mutual conversion between the sulfur in the sedimentary facies will produce H_2S gas. Therefore, it is of great significance to study the occurrence state of sulfur in the coal seam to explore the genesis of H_2S gas.

The sulfur in the coal seam occurs in the form of inorganic sulfur, organic sulfur, and elemental sulfur. The elemental sulfur comes from the original formation, and the content is very small and can be ignored. Organic sulfur in the coal seam is generally divided into primary organic sulfur and secondary organic sulfur. The primary organic sulfur is the inherent sulfur carried by the plant itself in the process of coal formation, and the secondary organic sulfur is the organic sulfur generated by biochemical action. The organic sulfur in coal is mostly secondary organic sulfur. Inorganic sulfur in the coal seam is divided into sulfate and iron sulfide sulfur. The results of the morphological sulfur analysis of the coal samples taken are shown in Table 4. The sulfur content of iron sulfide in no. 1−5 coal samples is higher. The sulfur of iron sulfide is mainly pyrite, supplemented by other sulfide minerals, and the sulfate sulfur is mainly gypsum and iron-containing sulfate, indicating that the coal seam is rich in pyrite.

Pyrite is the main form of inorganic sulfur, which is the product of the reaction between H_2S and active ferrous ions in coal seams. As shown in eq 4, it is mainly nodular in coal seams, and the size of nodules is generally 3−5 cm. There is a large amount of pyrite in the 13# coal seam of the Shaping mine.

$$2H_2S + Fe^{2+} \rightarrow FeS_2 + 2H^+ \quad (4)$$

The iron sulfide sulfur in the coal seam is mainly composed of pyrite. The iron sulfide sulfur in most of the 13# coal seams accounts for 50% or more of the total sulfur content. As shown in Figure 3, the high content of iron sulfide sulfur in the coal sample

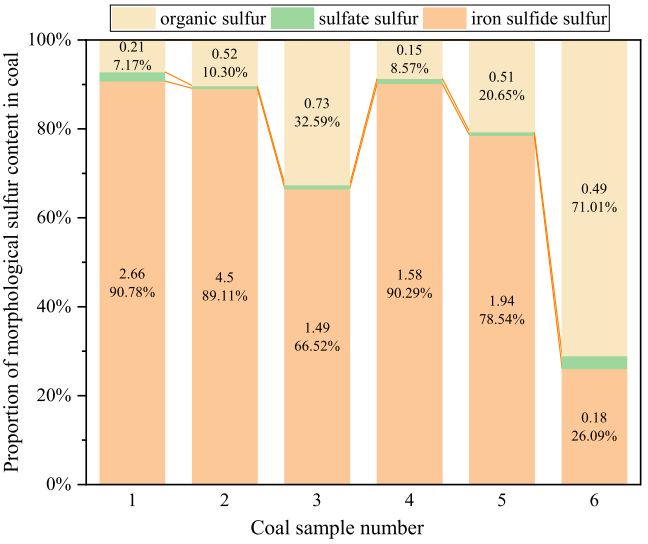

Figure 3. Proportion of sulfur content of each form in the coal sample.

indicates that coal seam pyrite is relatively developed. Pyrite is the product of the subsequent reaction of BSR, and the well-developed pyrite in the coal seam is the evidence of BSR.

The high content of pyrite in the coal seam is the direct evidence of the formation of H_2S by BSR because H_2S produced by BSR is fixed by Fe^{2+} in the coal seam to form pyrite. Under the action of BSR, sulfate in the coal seam is reduced by bacteria to form sulfur, and the sulfur isotope fractionation effect caused by bacterial alienation is more obvious. The average $\delta^{34}S$ value of pyrite in the coal seam is negative. The temperature of the coal seam is suitable for the reproduction of SRB. Combined with the pyrite rich in the coal seam, the cause of H_2S in the coal seam can be preliminary judged as BSR.

Table 4. Form of Sulfur Content in Various Coal Samples

coal sample number	total sulfur/%	sulfate sulfur/%	iron sulfide sulfur/%	organic sulfur/%
1	2.93	0.06	2.66	0.21
2	5.05	0.03	4.50	0.52
3	2.24	0.02	1.49	0.73
4	1.75	0.02	1.58	0.15
5	2.47	0.02	1.94	0.51
6	0.69	0.02	0.18	0.49

https://doi.org/10.1021/acsomega.3c09057
ACS Omega 2024, 9, 2980−2987

3.4. Analysis of Sulfur Isotope. As an effective tracer method to reveal the sulfur cycle process in the sedimentary system, the sulfur isotope has been widely used in judging the source of sulfur. Li[24,28] and other scholars proposed that the S contained in H_2S gas in a coal mine all came from sulfur-containing organic matter or sulfate products in the stratum, and the S cycle is completed in the conversion process of different forms of S, and finally, the fractionation process of sulfur isotopes is completed.

If the sulfur in coal comes from the secondary sulfur in the coal-forming process, then a large isotopic fractionation will occur under the action of SRB, resulting in a significant loss of $\delta^{34}S$ in this part of the sulfur isotope, and the sulfur isotope value is negative. The coal seams with little seawater influence are characterized by positive $\delta^{34}S$ values; the coal seams that are greatly affected by seawater have negative $\delta^{34}S$ values. H_2S formed for different reasons in the coal seams has different sulfur isotopes. The sulfur isotope measurement results of coal in different parts of the 13# coal seam are shown in Table 5. The

Table 5. Test Results of Coal-like Sulfur Isotopes

coal sample number	pyrite sulfur isotope ($\delta^{34}S$) values (‰)
1	−7.6
2	−8.2
3	−6.4
4	−7.9
5	−8.3
6	−7.7

sulfur isotope results of coal samples in 6 groups are all negative, and the $\delta^{34}S$ values in coal samples are distributed in the range of −8.3−6.4‰, which is consistent with the fractionation mechanism under the action of SRB in the coal formation process of this coal seam.

3.5. Water Sample Analysis. The surface water system of the Shaping mine belongs to the Yellow River basin. The river water level near the coal mine is relatively high, up to 842.46 m, and the annual average flow is as high as 823.04 m^3/s. The coal mine belongs to the tributary of the east bank of the Yellow River in the Yellow River Basin and the catchment area of the county river. The distribution of the surface water system around the coal mine is shown in Figure 4. The Xianchuan River is one of the tributaries on the eastern bank of the Yellow River. It is located 100 m outside the south of the coal mine. The river direction is from east to west, and its river branch extends to the

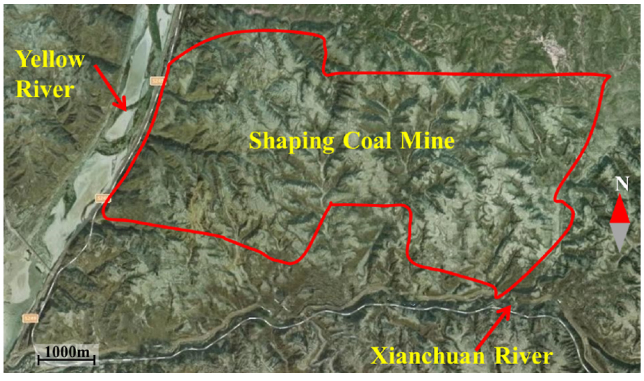

Figure 4. Distribution diagram of the surface water system in a coal mine.

south of Shaping mine, which is a seasonal river. The water system flowing through the coal mine is rich, and a large amount of minerals, such as sulfates, are dissolved, which provides a sufficient material basis for the generation of H_2S gas.

Tap water (group A) and coal seam water (group B) were taken as samples for detection. The concentrations of SO_4^{2-} and HCO_3^- in tap water and coal seam water samples are shown in Figure 5. The concentrations of SO_4^{2-} and HCO_3^- in the two

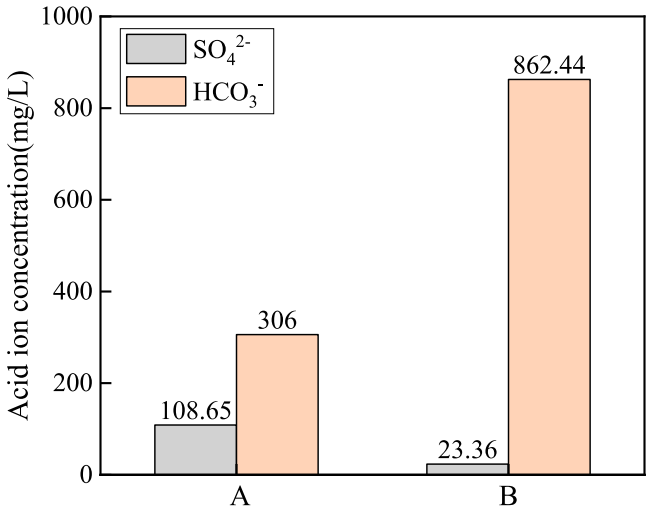

Figure 5. Distribution map of acid ion concentration in water samples.

groups of water samples are significantly different. The concentration of SO_4^{2-} in group A is 4.6 times higher than that in group B, while the concentration of HCO_3^- in the water sample of group B was much higher than that of group A.

The process of BSR producing H_2S gas requires water as the medium to participate in the reaction with the reactants. SO_4^{2-} in water participates in the BSR process as the main sulfur source, and the products are mainly H_2S gas and HCO_3^-, as shown in eq 5. The concentration of SO_4^{2-} in coal seam water is an important factor affecting the generation of H_2S gas. When the H_2S gas in the coal seam is abnormal, the SO_4^{2-} concentration in coal seam water is lower than that in tap water, and a large amount of SO_4^{2-} is consumed in the water during the BSR process, resulting in a low SO_4^{2-} concentration in the coal seam water.

$$2C + SO_4^{2-} + 2H_2O \xrightarrow{\text{sulfate-reducing bacteria}} H_2S\uparrow + HCO_3^- \quad (5)$$

BSR generated HCO_3^- and H_2S at the same time, and the concentration of HCO_3^- in the coal seam water indirectly expressed the reaction process. When the H_2S gas concentration in the coal seam is high, the HCO_3^- concentration in the coal seam water is higher than in tap water. It can be seen from Figure 5 that the concentration of SO_4^{2-} in the coal seam water sample is lower than that of tap water, but the concentration of HCO_3^- in the water sample is much higher than that of tap water, indicating that HCO_3^- is formed after the reaction of SO_4^{2-} in coal seam water, which further proves that the H_2S gas in the coal seam is caused by BSR.

https://doi.org/10.1021/acsomega.3c09057
ACS Omega 2024, 9, 2980−2987

4. DEDUCTION OF THE FORMATION PROCESS OF H_2S IN COAL SEAM

4.1. Deduction of the Origin of H_2S in Coal Seam. There is no magma intrusion or volcanic activity in the 13# coal seam of this mine, which excludes the possibility of the origin of magmatic activity. The vitrinite reflectance of the coal sample is between 0.45 and 0.70%, and the thermal evolution temperature of the coal seam is calculated to be between 51.47 and 108.12 °C, all less than 120 °C, which excludes TSR as the cause of H_2S gas. The coal mine is close to the Yellow River, and the coal-forming process experiences the alternation of land and sea, so the coal seam is rich in sulfate compounds and organic matter. The coal seam temperature range is 18.6−39.9 °C, which provides a suitable environment for the growth of reducing bacteria and meets the conditions for the occurrence of BSR.

The 13# coal seam with a high content of pyrite and its $\delta^{34}S$ value are all negative values; the concentration of SO_4^{2-} in the coal seam is low, and the concentration of HCO_3^- is high, which strongly proves that the H_2S gas in this coal seam is caused by BSR. The reasoning process is shown in Figure 6.

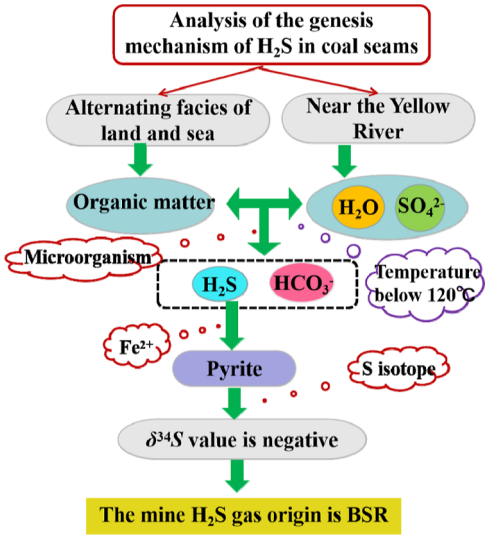

Figure 6. Reasoning diagram of H_2S formation in a coal seam.

4.2. Evolution History of Organic Sulfur in Coal Seam. The evolution process of sulfur in the coal seam is the formation and transformation of organic sulfur and inorganic sulfur, and H_2S gas will be produced in this process. Organic sulfur in coal seams includes primary organic sulfur and secondary organic sulfur. According to BSR action, the evolution history of organic sulfur in the coal seam is shown in Figure 7.

The primary organic sulfur in the 13# coal seam of Shaping mine mainly comes from the proteins of animal and plant remains in the original sedimentary environment. The production process of secondary organic sulfur is relatively complicated; after plants die and decompose, they form primary organic sulfur, H_2S, CH_3SH, and other sulfur-containing compounds. With the participation of oxygen, sulfur-containing compounds are finally oxidized to SO_4^{2-}, and a small portion exists in the form of sulfate. A large amount of SO_4^{2-} in coal seams and water is decomposed by microbial reduction to generate sulfur substances such as H_2S gas, as shown in eq 6. It is stored in the pores of coal.

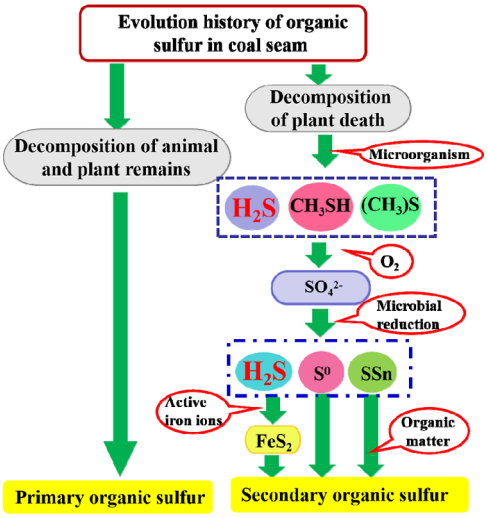

Figure 7. Evolution history of organic sulfur in a coal seam.

$$\sum CH + SO_4^{2-} + H_2O \xrightarrow{\text{microorganism}} H_2S\uparrow + CO_2\uparrow + CO_3^{2-} \quad (6)$$

H_2S reacts with the active iron ion in the coal seam to generate pyrite, as shown in eq 4. At the same time, part of the secondary organic sulfur will be generated, and the reaction of elemental sulfur and compound sulfur with organic matter will also produce secondary organic sulfur.

4.3. Evolution History of Pyrite in Coal Seams. In the 13# coal seam of this mine, pyrite is the main inorganic sulfur, and the content of sulfate minerals is low. H_2S gas is generated during the formation of pyrite in the coal seam. Pyrite in coal seams includes crystalline pyrite and complex pyrite. According to BSR action, the evolution history of pyrite in a coal seam is shown in Figure 8.

It can be seen from Figure 8 that the evolution process of pyrite in the coal seam is similar to that of organic sulfur, and there are also two stages of H_2S gas generation, which are the

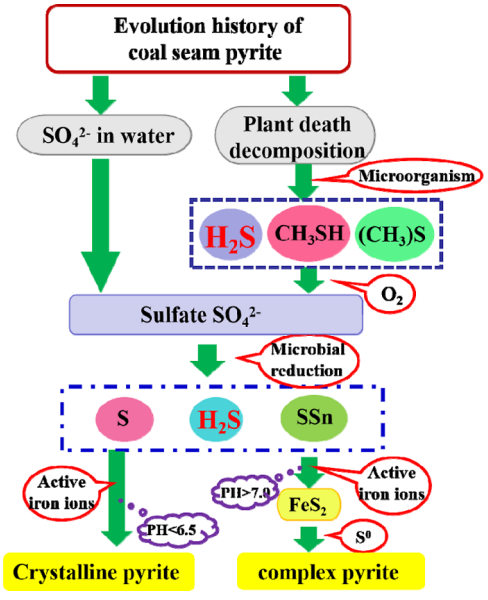

Figure 8. Evolution history of coal seam pyrite.

https://doi.org/10.1021/acsomega.3c09057
ACS Omega 2024, 9, 2980−2987

decomposition of plant death and the reduction of SO_4^{2-}. The formation of coal seam pyrite requires sulfate as the raw material, and the sulfate generated by the decomposition reaction of plant death or SO_4^{2-} in water is reacted by reducing bacteria to generate H_2S gas, trace element sulfur, and double sulfur. When the environment pH < 6.5 is weakly acidic, the active iron ions and H_2S gas undergo physic-chemical action to form crystalline pyrite; when the environment pH > 7 is weakly alkaline, the polysulfide reacts with iron ions to convert into FeS_2, with the participation of S, FeS_2 will further generate complex pyrite, and the reaction process is shown in eqs 7−9.

$$Fe^{2+} + H_2S + nH_2O \rightarrow FeS{\cdot}nH_2O + 2H^+ \quad (7)$$

$$2Fe^{3+} + 3H_2S \rightarrow 2FeS + S + 6H^+ \quad (8)$$

$$S + FeS{\cdot}nH_2O \rightarrow FeS_2{\cdot}nH_2O \rightarrow FeS_2 \quad (9)$$

4.4. Relationship between Hydrogen Sulfide and Sulfur in Coal Seam. Under the action of BSR, a large amount of sulfate in the coal seam is reduced by microorganisms to form H_2S. According to the evolution histories of organic sulfur (Figure 7) and pyrite (Figure 8) in the coal seam. It is speculated that H_2S and a substance in the coal seam are converted into organic sulfur and pyrite, which is mainly composed of iron sulfide sulfur and stored in the coal, resulting in a high content of organic sulfur and iron sulfide sulfur in the coal seam containing H_2S. So, sulfur in coal has a certain relationship with the occurrence of H_2S. The relationship between H_2S concentration and morphological sulfur content is shown in Figure 9.

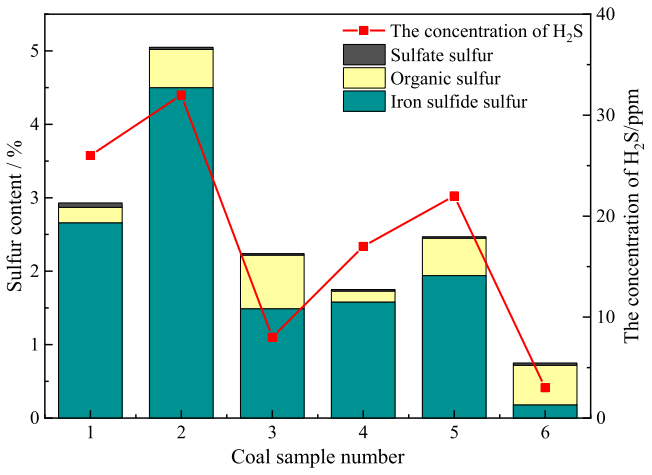

Figure 9. Plot of the H_2S concentration and morphological sulfur content in coal.

It can be seen from Figure 9 that the form of sulfur in the coal seam is mainly iron sulfide sulfur, followed by organic sulfur, and sulfate sulfur is the least, and the H_2S concentration has a similar change trend to iron sulfide. The H_2S gas in the coal seam is generated by the sulfate in the coal through the BSR action and reacts with organic matter and iron ions to generate organic sulfur and pyrite. In coal seams, the positions with high H_2S stocks also have large organic sulfur and pyrite content, indicating that there is a positive correlation between sulfur elements and H_2S gas concentration in coal.

5. CONCLUSIONS

(1) The highest temperature in the thermal evolution process of the coal seam is determined to be 108.12 °C by the vitrinite reflectance. The concentration of SO_4^{2-} in coal seam water is 0.2 times that of tap water, and the concentration of HCO_3^- is 2.8 times that of tap water, indicating that SO_4^{2-} in coal seam water is consumed to generate HCO_3^-.

(2) The sulfur content of iron sulfide in coal samples accounts for more than 50% of total sulfur, indicating that there is a lot of pyrite in coal-measure strata. The results of sulfur isotope detection in coal samples are all negative, indicating that the coal seam is greatly affected by seawater in the process of coal formation, the sulfur isotope fractionation is large, and the loss is significant.

(3) Based on the thermal evolution history, pyrite content in coal, sulfur isotope, and water sample analysis of the coal mine, it is concluded that the origin of the H_2S gas in the mine is BSR.

AUTHOR INFORMATION

Corresponding Author

Siqi Wang − *College of Safety Science and Engineering, Liaoning Technical University, Huludao 125000, China; Key Laboratory of Thermal Disaster and Prevention, Ministry of Education, Huludao 125000, China;* orcid.org/0009-0003-1914-1591; Email: 18241847929@163.com

Authors

Chunming Ai − *College of Safety Science and Engineering, Liaoning Technical University, Huludao 125000, China; Key Laboratory of Thermal Disaster and Prevention, Ministry of Education, Huludao 125000, China*

Pingping Sun − *College of Safety Science and Engineering, Liaoning Technical University, Huludao 125000, China; Key Laboratory of Thermal Disaster and Prevention, Ministry of Education, Huludao 125000, China*

Shuyu Zhao − *Shanxi Jinshen Shaping Coal Industry Co., Ltd., Xinzhou 036500 Shanxi, China*

Xiaozhi Mu − *Shanxi Jinshen Shaping Coal Industry Co., Ltd., Xinzhou 036500 Shanxi, China*

Complete contact information is available at: https://pubs.acs.org/10.1021/acsomega.3c09057

Notes

The authors declare no competing financial interest.

ACKNOWLEDGMENTS

The authors greatly acknowledge the financial support from the National Natural Science Foundation of China (51604138) and the Natural Science Foundation Program of Liaoning Province (no. 2022-MS-395).

REFERENCES

(1) Hu, W.; Huang, J.; Wang, J.; Xie, D.; Wang, Z.; Qiao, Y.; Xu, M. Benign-by-design N-doped activated carbon from wasted aqueous assisted hydrochar of leftover rice for efficient H_2S removal. *Fuel* **2024**, *358*, 130233.

(2) Xian, S.; Xu, Q.; Li, H. Mechanism Insight into the Conversion between H_2S and Thiophene during Coal Pyrolysis: A Theoretical Study. *ACS Omega* **2023**, *8* (37), 33982−33996.

(3) Sun, J.; Li, L.; Zhou, G.; Wang, X.; Zhang, L.; Liu, Y.; Yang, J.; Lü, X.; Jiang, F. Biological sulfur reduction to generate H_2S as a reducing agent to achieve simultaneous catalytic removal of SO_2 and NO and sulfur recovery from fue gas. *Environ. Sci. Technol.* **2018**, *52* (8), 4754−4762.
(4) Li, X.; Krooss, B. M.; Ostertag-Henning, C.; Weniger, P.; Littke, R. Liberation of hydrogen-containing gases during closed system pyrolysis of immature organic matter-rich shales. *Int. J. Coal Geol.* **2018**, *185*, 23−32.
(5) Weiji, S.; Xinpeng, Y.; Bing, L.; Xiuyu, Z.; Lei, Z. Injecting $NaHCO_3$ solution into coal seam to control hydrogen sulfide: method and effects. *China Saf. Sci. J.* **2016**, *26* (01), 104−108.
(6) Zhonghui, M. Study on occurrence mechanism and treatment of hydrogen sulfide in some coal mines in Xinjiang. *Coal Eng.* **2017**, *49* (S2), 131−133.
(7) State Administration of Work Safety. *Coal Mine Safety Regulations*; Coal Industry Press, 2016.
(8) Haifei, L.; Jinggei, Z.; Shugang, L.; Chao, Z.; Huijun, Y. Generalized grey relational analysis on main controlling factors for abnormal enrichment of hydrogen sulfide in thecoal mine. *J. Saf. Sci. Technol.* **2017**, *13* (06), 27−33.
(9) Deng, Q.; Yin, J.; Wu, X.; Zhang, T.; Wang, H.; Liu, M. Research Advances of Prevention and Control of Hydrogen Sulfide in Coal Mines. *Sci. World J.* **2019**, *2019*, 1−15.
(10) Wei, W.; Baoshan, J.; Yun, Q. Research and application of hydrogen sulfide control technology with enclosed air curtain in fully-mechanized excavation face. *China Saf. Sci. J.* **2017**, *13* (06), 27−33.
(11) Hosseiny, E.; Baniasad, A. R.; Dehyadegari, E. The genesis of H_2S associated with heavy oils in Hendijan and Bahregansar oilfields, Sarvak reservoir. *Energy Sources, Part A* **2016**, *38* (8), 1140−1147.
(12) Yongjie, Y.; Xuan, L.; Chao, Y.; et al. Study on hydrogen sulfide adsorption by MOFs loaded polyvinyl imine (PEI). *Coal J.* **2023**, 1−11.
(13) de Oliveira Carneiro, L.; de Vasconcelos, S. F.; de Farias Neto, G. W.; Brito, R. P.; Brito, K. D. Improving H2S removal in the coke oven gas purification process. *Sep. Purif. Technol.* **2021**, *257*, 117862.
(14) Li, P.; Li, B.; Duan, J.; Zhao, Y.; Zou, H.; Hao, F. Sulfate sources of thermochemical sulfate reduction and hydrogen sulfide distributions in the Permian Changxing and Triassic Feixianguan formations, Sichuan Basin, SW China. *Mar. Pet. Geol.* **2022**, *145*, 105892.
(15) Xie, W.; Wang, H.; Wang, M.; He, Y. Genesis, controls and risk prediction of H_2S in coal mine gas. *Sci. Rep.* **2021**, *11* (1), 5712.
(16) Deng, Q.; Li, S.; Yao, M.; Liu, C.; Zhang, Z.; Xiang, S. Study on the factors of hydrogen sulfide production from lignite bacterial sulfate reduction based on response surface method. *Sci. Rep.* **2023**, *13* (1), 20537.
(17) Gao, F.; Jia, Z.; Xia, J.; Wang, D.; Yang, Y.; Shan, Y.; Shen, J. Study on H_2S Occurrence in Low Sulfur Coal Seams. *Adsorpt. Sci. Technol.* **2022**, *2022*, 1−11.
(18) Dao, Y.; Zhou, J. X.; Wang, X. H.; Zhang, Y. H.; Liu, H. S.; Sun, G. T.; Yue, Z. P.; He, Y. Selenium enrichment in the Dingtoushan carbonate-hosted epigenetic Pb-Zn deposit in the western Yangtze Block, SW China. *Ore Geol. Rev.* **2023**, *163*, 105736−105814.
(19) Yufen, W. Analysis of hydrogen sulfide origin for coal seams of the Taiyuan formation in Tiexin mine field. *J. Liaoning Tech. Univ.* **2015**, *34* (10), 1137−1142.
(20) Asaoka, S.; Endo, T.; Ushihara, Y.; Umehara, A.; Yogi, C.; Ohta, T.; Hayakawa, S.; Shutoh, N.; Okuda, T. Spatial and temporal distribution of hydrogen sulfide and sulfur species in coastal marine sediments collected from Osaka Bay, Japan. *Mar. Chem.* **2023**, *251*, 104233.
(21) Cheng, Y.; Feng, Z.; Guo, C.; Chen, P.; Tan, C.; Shi, H.; Luo, X. Links of hydrogen sulfide content with fluid components and physical properties of carbonate gas reservoirs: A case study of the right bank of Amu Darya, Turkmenistan. *Front. Earth Sci.* **2022**, *10*, 910666.
(22) Dongna, L.; Meiling, M. Application and progress of vitrinite reflectance method for calculation of paleo Geo-Temperature and restoration of eroded strata thickness. *J. Taiyuan Univ. Technol.* **2014**, *45* (05), 643.
(23) Zhu, G.; et al. Sulfur isotopic fractionation and mechanism for thermochemical sulfate reduction genetic H_2S. *Acta Petrol. Sin.* **2014**, *30* (12), 3772−3786.
(24) Li, Z.; et al. Geochemistry characteristics of hydrogen sulphide-bearing gas pools in Sichuan Basin. *Energy Explor. Exploit.* **2014**, *32*, 691.
(25) Kokh, M. A.; Assayag, N.; Mounic, S.; Cartigny, P.; Gurenko, A.; Pokrovski, G. S. Multiple sulfur isotope fractionation in hydrothermal systems in the presence of radical ions and molecular sulfur. *Geochim. Cosmochim. Acta* **2020**, *285*, 100−128.
(26) Zheng, X.; et al. Distribution of gypsum and sulfur isotopes in the Palaeogene strata, western Qaidam Basin, Qinghai. *Sediment. Geol. Tethyan Geol.* **2019**, *39* (04), 65−70.
(27) Chang, J.; Yang, L.; Li, C.; Qiu, N.; Zhang, H.; Wang, X. Tectono-thermal evolution of the northern Tarim Basin, Central Asia: new insights from apatite low-temperature thermochronometers. *J. Asian Earth Sci.* **2024**, *259*, 105919.
(28) Ketrov, A. A.; Yudovskaya, M. A.; Shelukhina, Y. S.; Velivetskaya, T. A.; Palamarchuk, R. S. Sources and Evolution of Sulfur Isotopic Composition of Sulfides of the Kharaelakh and Pyasino-Vologochan Intrusions, Norilsk Ore Region. *Geol. Ore Deposits* **2022**, *64* (6), 350−376.

https://doi.org/10.1021/acsomega.3c09057
ACS Omega 2024, 9, 2980−2987